Engineering 37 (2024) 27–39

Contents lists available at ScienceDirect

Engineering

journal homepage: www.elsevier.com/locate/eng

Research
Emerging Contaminant Control: Science and Technology—Review

UV-Based Advanced Oxidation Processes for Antibiotic Resistance Control: Efficiency, Influencing Factors, and Energy Consumption

Jiarui Han [a,#], Wanxin Li [a,#], Yun Yang [a], Xuanwei Zhang [a], Siyu Bao [a], Xiangru Zhang [a,*], Tong Zhang [b], Kenneth Mei Yee Leung [c]

[a] Department of Civil and Environment Engineering, The Hong Kong University of Science and Technology, Hong Kong 999077, China
[b] Department of Civil Engineering, The University of Hong Kong, Hong Kong 999077, China
[c] State Key Laboratory of Marine Pollution and Department of Chemistry, City University of Hong Kong, Hong Kong 999077, China

ARTICLE INFO

Article history:
Received 30 January 2023
Revised 19 September 2023
Accepted 19 September 2023
Available online 15 December 2023

Keywords:
Advanced oxidation processes
Ultraviolet/chlorine
Ultraviolet/hydrogen peroxide
Ultraviolet/persulfate
Antibiotic resistant bacteria
Antibiotic resistance genes

ABSTRACT

Antibiotic resistant bacteria (ARB) with antibiotic resistance genes (ARGs) can reduce or eliminate the effectiveness of antibiotics and thus threaten human health. The United Nations Environment Programme considers antibiotic resistance the first of six emerging issues of concern. Advanced oxidation processes (AOPs) that combine ultraviolet (UV) irradiation and chemical oxidation (primarily chlorine, hydrogen peroxide, and persulfate) have attracted increasing interest as advanced water and wastewater treatment technologies. These integrated technologies have been reported to significantly elevate the efficiencies of ARB inactivation and ARG degradation compared with direct UV irradiation or chemical oxidation alone due to the generation of multiple reactive species. In this study, the performance and underlying mechanisms of UV/chlorine, UV/hydrogen peroxide, and UV/persulfate processes for controlling ARB and ARGs were reviewed based on recent studies. Factors affecting the process-specific efficiency in controlling ARB and ARGs were discussed, including biotic factors, oxidant dose, UV fluence, pH, and water matrix properties. In addition, the cost-effectiveness of the UV-based AOPs was evaluated using the concept of electrical energy per order. The UV/chlorine process exhibited a higher efficiency with lower energy consumption than other UV-based AOPs in the wastewater matrix, indicating its potential for ARB inactivation and ARG degradation in wastewater treatment. Further studies are required to address the trade-off between toxic byproduct formation and the energy efficiency of the UV/chlorine process in real wastewater to facilitate its optimization and application in the control of ARB and ARGs.

© 2023 THE AUTHORS. Published by Elsevier LTD on behalf of Chinese Academy of Engineering and Higher Education Press Limited Company. This is an open access article under the CC BY license (http://creativecommons.org/licenses/by/4.0/).

1. Introduction

Antibiotics are considered one of the most momentous inventions in pharmaceutical science because antibiotics effectively treat bacterial infections and increase life expectancy [1]. Globally, antibiotic consumption has been estimated at 100 000–200 000 tonnes per year [2], and the use of antibiotics continues to rise. A survey of antibiotic consumption in 76 countries revealed that antibiotic consumption increased by 65% from 2000 to 2015 [3]. Antibiotic resistance occurs naturally when bacteria evolve to become resistant to the effects of antibiotics [4]. However, anthropogenic activities, including misuse or overuse of antibiotics, greatly promote the selection of antibiotic resistant bacteria (ARB) and antibiotic resistance genes (ARGs) [5,6]. Antibiotic resistance threatens the efficacy of antibiotics in treating infectious diseases, resulting in longer hospital stays, higher therapeutic costs, and higher morbidity and mortality rates [5,7,8]. It was predicted that ten million people would die annually by 2050 as a result of antimicrobial resistance [9]. The World Health Organization has declared that antibiotic resistance is one of the most severe threats to public health in the 21st century [9].

Intrinsic resistance, genetic mutations, vertical gene transfer, and horizontal gene transfer have been reported as primary mechanisms for the development and spread of antibiotic resistance [10,11]. Intrinsic resistance is related to actions such as the prevention of antibiotic entry into the cytoderm, expulsion of specific

* Corresponding author.
E-mail address: xiangru@ust.hk (X. Zhang).
# The authors contributed equally to this work.

https://doi.org/10.1016/j.eng.2023.09.021
2095-8099/© 2023 THE AUTHORS. Published by Elsevier LTD on behalf of Chinese Academy of Engineering and Higher Education Press Limited Company.
This is an open access article under the CC BY license (http://creativecommons.org/licenses/by/4.0/).

antibiotics by explicit efflux pumps before they reach their targets, and degradation or even deactivation of antibiotics. Mutagenesis leads to antibiotic resistance in several ways, including switching antibiotic targets, medically altering enzymes, increasing drug efflux, and decreasing target gene expression [12]. Vertical gene transfer means that the genetic material is inherited from parental cells and occurs only when microbial gene portability is possible for transfer to the daughter cells [13]. Although the level of extracellular ARGs (e-ARGs) is typically 2–3 orders of magnitude lower than that of intracellular ARGs (i-ARGs), the spread of e-ARGs could be significantly enhanced by horizontal gene transfer [10,14]. Horizontal gene transfer can occur through gene transfer agents, conjugation, transformation, and transduction (Fig. 1 [10,15]). Gene transfer agents are virus-like elements that transfer parts of DNA from host cells to recipient cells or free particles that spread to recipient cells by cell lysis [10]. Conjugation occurs when cell-to-cell contact causes ARGs carried by mobile genetic elements to be delivered from donor to recipient cells [16]. In the transformation process, naturally transformable bacteria uptake, integrate, and functionally express e-ARGs. In the transduction process, i-ARGs from a donor cell are packaged into bacteriophages when DNA replication begins, and ARGs carried by bacteriophages are combined with the genome of recipient cells once they are infected by bacteriophages [17]. The multiple mechanisms for the emergence and dissemination of antibiotic resistance highlight the challenges in controlling ARB and ARGs [15,18].

It has been reported that approximately 50%–90% of human and veterinary antibiotics and their metabolites are excreted in their active forms via urine and feces [19]. Wastewater containing antibiotics from households, livestock farms, and hospitals continuously enters wastewater treatment plants [20], where most antibiotics are inefficiently removed or deactivated by traditional wastewater treatment processes [21,22]. At the same time, activated sludge used in the biological treatment unit has high microbial density and diversity, which favors horizontal gene transfer [23]. With relatively high levels of antibiotics and substantial amounts of activated sludge biomass, wastewater treatment plants have been reported to be hotspots for promoting the proliferation of ARB and ARGs [24,25]. For instance, the relative abundance of *tet* genes in wastewater effluents increased by 212%–358% after biological treatment [24]. Due to the insufficient removal efficiency of conventional wastewater treatment, significant amounts of antibiotics, ARB, and ARGs may enter aquatic environments [25,26]. As a result, the occurrence of ARB and ARGs from wastewater to drinking water sources has been frequently detected [24–29]. Recently, Zhang et al. [4] collected 4572 metagenomic samples from the European Nucleotide Archive to determine the global distribution of ARGs, among which 1819 samples were from wastewater and aquatic environments. A total of 2561 ARGs that collectively conferred resistance to 24 classes of antibiotics were identified. Only 25 ARGs were detected with an occurrence frequency of higher than 75%, and the frequency of most ARGs was less than 10%. The abundance of ARGs in aquatic environments varied markedly, ranging from less than 0.005 to 296 reads per kilobase per million per sample. By considering the occurrence frequency and abundance of ARGs and other factors such as the potential of contributing to pathogenicity, ARGs with relatively high health risks were determined and are listed in Table 1 [4].

Ultraviolet (UV) and chemical oxidants (e.g., chlorine) are commonly used in water and wastewater treatment for disinfection, which is considered the last and most solid barrier to control microbial risks [30]. To inactivate ARGs, higher UV doses are required than those used in standard disinfection practices [26,31]. However, there is evidence that UV and chemical oxidation might enrich ARB and ARGs in finished water/wastewater [28,32–35]. For instance, drinking water chlorination was found to increase the absolute abundance of 14 of the 18 ARG subtypes [36]. In a full-scale wastewater treatment plant, chlorination was found to increase the absolute abundance of e-ARGs by up to 3.8 times and i-ARGs by 7.8 times [33]. Yuan et al. [34] reported that chlorination increased the transformation frequency of e-ARGs by 2.9–7.2 times because chlorination resulted in cell debris with enhanced adsorption of e-ARGs and thus increased their persistence and propagation potential. UV treatment was found to increase the relative abundance of 159 ARGs in wastewater by 6.0 times [32]. In addition, ARB may regenerate and reactivate in water/wastewater treated with UV or chemical oxidants [37,38]. Such regrowth of damaged cells may lead to horizontal gene transfer and the spread of antibiotic resistance [39], further compromising the microbial safety of water/wastewater. These findings indicate that treatment by UV irradiation or chemical oxidation alone is not adequate for effectively inactivating ARB and degrading ARGs.

In recent years, controlling the risks of ARB and ARGs in aquatic environments with UV-based advanced oxidation processes (AOPs) has gained increasing interest, as these processes have been reported to significantly promote the reduction of ARB and ARGs due to the rapid formation of reactive species [40–48]. The application and performance of UV-based advanced treatments in controlling ARB and ARGs have been previously reviewed [31,49]. In this

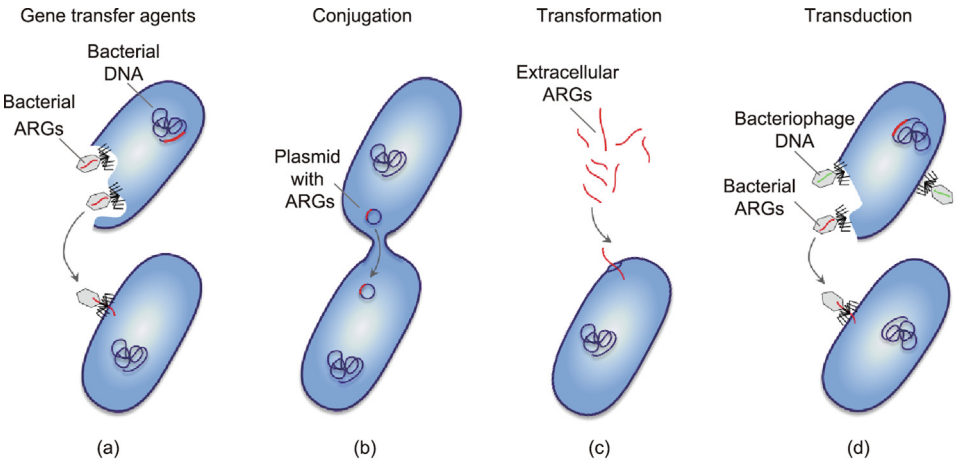

Fig. 1. Mechanisms of horizontal gene transfer: (a) gene transfer agents; (b) conjugation; (c) transformation; and (d) transduction [10,15].

Table 1
ARGs with relatively high health risks [4].

Health risk ranking	ARG	Category	Health risk ranking	ARG	Category
1	*ermB*	Macrolide–lincosamide–streptogramin (MLS) resistant	26	*APH(6)-Id*	Aminoglycoside resistant
2	*acrB*	Multidrug resistant	27	*APH(3″)-Ib*	Aminoglycoside resistant
3	*marA*	Multidrug resistant	28	*ermF*	MLS resistant
4	*H-NS*	Multidrug resistant	29	*mgrA*	Multidrug resistant
5	*acrF*	Multidrug resistant	30	*msrA*	Multidrug
6	*evgS*	Multidrug resistant	31	*emrB*	Fluoroquinolone resistant
7	*acrE*	Multidrug resistant	32	*tet(A)*	Tetracycline resistant
8	*acrS*	Multidrug resistant	33	*oqxB*	Multidrug resistant
9	*evgA*	Multidrug resistant	34	*mdtH*	Fluoroquinolone resistant
10	*CRP*	Multidrug resistant	35	*mphA*	MLS resistant
11	*mdtE*	Multidrug resistant	36	*mphC*	MLS resistant
12	*mdtF*	Multidrug resistant	37	*ermX*	MLS resistant
13	*tolC*	Multidrug resistant	38	*efrA*	Multidrug resistant
14	*gadX*	Multidrug resistant	39	*qacA*	Fluoroquinolone resistant
15	*gadW*	Tetracycline resistant	40	*mel*	Multidrug resistant
16	*tetO*	Tetracycline resistant	41	*oqxA*	Multidrug resistant
17	*tetM*	Multidrug resistant	42	*cfxA2*	Beta-lactams resistant
18	*mdtM*	Fluoroquinolone resistant	43	*AAC(6′)-Ie-APH(2″)-Ia*	Aminoglycoside resistant
19	*emrR*	Tetracycline resistant	44	*acrD*	Aminoglycoside resistant
20	*emrY*	Multidrug resistant	45	*tet(40)*	Tetracycline resistant
21	*tetQ*	Tetracycline resistant	46	*cfxA3*	Beta-lactams resistant
22	*tetW*	Tetracycline resistant	47	*mexB*	Multidrug resistant
23	*emrK*	Tetracycline resistant	48	*ANT(2″)-Ia*	Aminoglycoside resistant
24	*tetB*	Tetracycline resistant	49	*tetX*	Tetracycline resistant
25	*emrA*	Fluoroquinolone resistant	50	*tet(X4)*	Tetracycline resistant

study, a systematic literature review of the state of the art of ARB/ARG control by UV-based AOPs was conducted. UV-based AOPs mainly include UV/hydrogen peroxide (H_2O_2), UV/chlorine, UV/persulfate, UV/ozone, and UV/catalyst processes. Few studies have been reported on ARB/ARG treatment with UV/ozone and UV/catalyst processes [43,50–53], and therefore this study focused on UV/H_2O_2, UV/chlorine, and UV/persulfate processes. The efficiencies and mechanisms of the three UV-based AOPs in inactivating ARB and degrading ARGs under various environmental and operational conditions were discussed, with emphasis on improving the fundamental understanding of ARB and ARG control and providing guidelines for the engineering design of UV-based AOPs. Moreover, the cost-effectiveness of the three UV-based AOPs was systematically evaluated and compared based on the concept of electrical energy per order (EE/O), which may provide decision-makers with useful insights for selecting appropriate UV-based AOPs for practical application.

2. Inactivation of ARB and degradation of ARGs by UV-based AOPs

2.1. Efficiencies and mechanisms of UV-based AOPs in ARB inactivation and ARG degradation

The UV/chlorine process is gaining interest as an AOP due to its ease of implementation and high efficiency in degrading recalcitrant micropollutants, including ARB and ARGs [54–56]. Table 2 [44,56–60] shows data for ARB inactivation and ARG reduction in the combined UV/chlorine, UV alone, and chlorination alone. UV/chlorine has shown a robust capability of inactivating different kinds of ARB, with higher efficiencies than the summed efficiencies of UV alone and chlorination alone [49,57]. Synergistic effects were also found for ARG degradation using the UV/chlorine treatment. Compared with chlorine (20 $mg{\cdot}L^{-1}$) or UV_{254} (9.03 $mW{\cdot}cm^{-2}$) alone, 40 min of UV/chlorine treatment increased the degradation of *tetM* and *blaTEM* by 0.98–3.20 log and 1.28–3.36 log, respectively, in phosphate-buffered saline (PBS) [57]. In wastewater treatment plants, the combination of UV_{254} (0.1 $mW{\cdot}cm^{-2}$) and chlorination (2 $mg{\cdot}L^{-1}$) achieved an additional 1.4 log ARB in 1.3 min and 1.0–1.5 log ARG reduction in 53 min [60]. Furthermore, regrowth and reactivation of ARB were significantly inhibited by UV/chlorine treatment.

The UV/H_2O_2 process has also been extensively investigated to mitigate the risks associated with ARB and ARGs in aquatic environments [61–63]. In a 30 min UV_{254} (9.85 $mW{\cdot}cm^{-2}$)/H_2O_2 (340 $mg{\cdot}L^{-1}$) treatment, the abundances of target ARGs (*sul1*, *tetX*, *tetG*, and *intI1*) in wastewater were significantly reduced by 1.55–2.32 log [64]. Michael et al. [65] also reported substantial reductions of target ARGs (i.e., 2.0–3.7 log reduction of *sul1*, *sul2*, *tetM*, *blaOXA-A*, and *blaTEM*) by a 90 min UV_{254} (3.46 $mW{\cdot}cm^{-2}$)/H_2O_2 (5 $mg{\cdot}L^{-1}$) treatment. In contrast, an insignificant reduction in the abundances of target ARGs (including *blaTEM*, *qnrS*, and *tetW*) was observed by up to 240 min $UV_{320–450}$ (17.4 $\mu W{\cdot}cm^{-2}$)/H_2O_2 (20 $mg{\cdot}L^{-1}$) treatment of wastewater [66]. As shown in Table 3 [41,45,62–69], relatively high UV fluence and chemical doses were required for effective ARB inactivation and ARG degradation by UV/H_2O_2 treatment, while the efficiency was still higher than that of the H_2O_2 alone or UV alone process. The UV/H_2O_2 process has been shown to significantly inhibit the photoactivation and regeneration of bacteria [70].

Activation of persulfate, including peroxydisulfate (PDS) and peroxymonosulfate (PMS), by UV irradiation has shown promising potential to combat ARB and ARGs [45–47,71]. For instance, the UV_{254} (2.3 $\mu W{\cdot}cm^{-2}$)/PDS (238 $mg{\cdot}L^{-1}$) process was more effective than the UV_{254} (2.3 $\mu W{\cdot}cm^{-2}$)/H_2O_2 (34 $mg{\cdot}L^{-1}$) process in removing *blaKPC-3* in wastewater, and the two processes resulted in 80% and 67% reductions in 1 min, respectively [45]. For a 5 min treatment, both UV_{254}/PDS and UV_{254}/H_2O_2 treatments achieved higher than 98% degradation of the *blaKPC-3* gene. UV_{254} (100 $\mu W{\cdot}cm^{-2}$)/PMS (20 $mg{\cdot}L^{-1}$) treatment was found to reduce *sul1* and *intI1* levels by 2.9 log and 3.4 log, respectively, in 30 min [42]. The treatment efficiencies of ARB and ARGs using UV_{254}/PDS and UV_{254}/PMS under various operational conditions are listed in Table 4 [42,45–48,71–73]. The combination of UV_{254} and persulfate has been reported to effectively inactivate different types of ARB (e.g., antibiotic-resistant *Escherichia coli* (*E. coli*), *Klebsiella pneumoniae* (*K. pneumonia*), and *Pseudomonas* sp. HLS-6), and synergistic

Table 2
Performance of UV, chlorination, and the combined UV/chlorine treatment in ARB inactivation and ARG degradation.

Treatment	Target ARB	Target ARG	Reduction of ARB/ARGs (log)			Reference
			UV	Chlorine	UV/chlorine	
UV_{254}: 0.20 mW·cm^{-2} Chlorine: 20 mg·L^{-1} Time: 1 min Matrix: PBS	*Pseudomonas* sp. HLS-6	—	3	> 5	> 5	[44]
UV_{254}: 0.20 mW·cm^{-2} Chlorine: 20 mg·L^{-1} Time: 5 min Matrix: PBS	—	*sul1* *intI1*	0.51 0.78	1.77 2.46	3.30 3.69	
UV_{254}: 0.08 mW·cm^{-2} Chlorine: 20 mg·L^{-1} Time: 60 min Matrix: PBS	—	*sul1*	0.90	< 0.10	1.46	[56]
UV_{254}: 9.03 mW·cm^{-2} Chlorine: 1 mg·L^{-1} Time: 3 min Matrix: PBS	Tetracycline resistant *Escherichia coli* (*E. coli*) Amoxicillin resistant *E. coli*	— —	3.03 2.67	5.07 5.91	5.55 4.89	[57]
UV_{254}: 9.03 mW·cm^{-2} Chlorine: 20 mg·L^{-1} Time: 40 min Matrix: PBS	— —	*tetM* *blaTEM*	0.91 0.96	1.45 2.45	3.20 3.36	
UV_{254}: 0.20 mW·cm^{-2} Chlorine: 6 mg·L^{-1} Time: 1 min Matrix: wastewater	Total culturable bacteria	—	—	—	> 2	[58]
UV_{254}: 0.20 mW·cm^{-2} Chlorine: 6 mg·L^{-1} Time: 10 min Matrix: wastewater	Detected ARGs	—	—	—	1.36	
UV_{254}: 0.93 mW·cm^{-2} Chlorine: 2.5 mg·L^{-1} Time: 0.5 min Matrix: wastewater	Total coliform	—	3.2	—	> 5.4	[59]
UV_{254}: 0.10 mW·cm^{-2} Chlorine: 1 mg·L^{-1} Time: 1.3 min Matrix: wastewater	*Enterococcus faecalis*	—	2.2	< 0.1	3.10	[60]
UV_{254}: 0.10 mW·cm^{-2} Chlorine: 1 mg·L^{-1} Time: 53 min Matrix: wastewater	— — —	*strB* *tetA* *tetB*	0.89 1.37 1.62	1.4 0.9 1.1	1.42 1.74 1.99	

effects were observed compared with individual UV or persulfate treatment [45–47]. However, the superiority of the combined process over the individual UV_{254} or persulfate process varied for different ARGs. Zhou et al. [46] observed that UV_{254} (0.4 μW·cm^{-2})/PDS (238 mg·L^{-1}) treatment achieved a higher total ARG reduction level (3.84 log) than the UV_{254} irradiation (3.28 log) and PDS oxidation (1.68 log). Specifically, 83.4% of macrolide resistance genes were degraded by UV_{254}/PDS, which was significantly higher than the 68.5% reduction by UV_{254} irradiation and the 35.9% reduction by PDS oxidation. In contrast, the combined UV/PDS process improved the degradation of quinolone resistance genes by less than 5% compared with UV irradiation alone [46].

Compared to UV irradiation or chemical oxidation alone, the generally higher reduction of ARB and ARGs achieved by the UV-based AOPs has been reported to relate with the enhanced destruction of the spore surface and the distinct release of intracellular materials from ARB [61,72]. Effective damage to cell membrane integrity by UV-based AOPs promoted the inactivation of ARB and inhibited their regrowth. Fig. 2 [40,74] shows a schematic illustration of how ARB and ARGs are removed by UV-based AOPs. Although UV light can damage cell wall macromolecules, the main mechanism of bacterial inactivation by UV irradiation is to cause DNA double-strand breakage and chromosome aberration, leading to cell death by necrosis or apoptosis [75]. Chemical oxidants have been reported to inactivate bacteria primarily by damaging the cell surface and altering membrane permeability [76], with chlorine having a higher disinfection potency than H_2O_2 and persulfate [77,78]. During the UV/chlorine, UV/H_2O_2, or UV/persulfate process, multiple radicals can be generated (Fig. 2, detailed in Section 2.2). The generated radicals are highly oxidative and can cause pronounced cell surface damage and increased cell permeability [74,79], which may facilitate the reaction of oxidants and free radicals with ARG-encoding DNA and promote DNA damage by UV irradiation [13]. Meanwhile, the increased cell permeability allows i-ARGs to be released into aquatic environments and converted into e-ARGs. It has been shown that compared with i-ARGs, e-ARGs are more likely to be degraded because they are more readily exposed to UV irradiation, chemical oxidants, and free radicals in the UV-based AOPs [79–81].

2.2. Formation and roles of reactive species

As described in Eqs. (1)–(6), multiple active oxidants are produced in the UV/chlorine process, including hydroxyl radicals ($^{\bullet}OH$) and reactive chlorine species (RCS) such as $Cl^{\bullet}$, $Cl_2^{\bullet-}$, and $ClO^{\bullet}$ (Fig. 2) [31]. The contributions of different radicals in the treatment of ARB and ARGs have been studied by using radical scavengers such as nitrobenzene (NB) for $^{\bullet}OH$ scavenging (the reaction rate constant $k_{OH-NB} = 3.9 \times 10^9\ L \cdot mol^{-1} \cdot s^{-1}$) in the UV/chlorine process. The addition of nitrobenzene resulted in little change in the log reduction of ARGs, indicating that $^{\bullet}OH$

Table 3
Performance of UV, H_2O_2, and the combined UV/H_2O_2 treatment in ARB inactivation and ARG degradation.

Treatment	Target ARB	Target ARG	Reduction of ARB/ARGs (log)			Reference
			UV	H_2O_2	UV/H_2O_2	
UV_{254}: 12 mJ·cm^{-2} H_2O_2: 3400 mg·L^{-1} Time: 60 min Matrix: PBS	*Staphylococcus aureus* *Pseudomonas aeruginosa* *(P. aeruginosa)*	—	2.5 2.5	0.2 0.3	3.7 3.6	[67]
UV_{254}: 120 mJ·cm^{-2} H_2O_2: 3400 mg·L^{-1} Time: 60 min Matrix: PBS	— —	*mecA* *ampC*	1.4 2.3	0.1 0.2	2.7 2.9	
UV_{254}: 0.3 mW·cm^{-2} H_2O_2: 10 mg·L^{-1} Time: 3 min Matrix: PBS	— —	i-*ampR* e-*ampR*	1.64 2.57	— —	1.48 4.91	[41]
UV_{254}: 1 mW·cm^{-2} H_2O_2: 50 mg·L^{-1} Time: 10 min Matrix: PBS	—	i-*gyrA*, i-*tetA*, i-*qnrS*, and i-*intI1*	1.32–4.74	—	1.02–5.22	[63]
UV_{254}: 1 mW·cm^{-2} H_2O_2: 50 mg·L^{-1} Time: 10 min Matrix: wastewater	— —	i-*gyrA*, i-*tetA*, i-*qnrS*, i-*intI1* e-*gyrA*, e-*tetA*, e-*qnrS*, and e-*intI1*	1.98–5.16 1.74–5.64	— —	2.34–5.58 1.68–5.64	
UV_{254}: 0.25 mW·cm^{-2} H_2O_2: 10 mg·L^{-1} Time: 21.3 min Matrix: PBS	*Pseudomonas putida* (*P. putida*) MX-2 —	— *P. putida* MX-2 carried ARGs	6.97 1.8	— —	6.97 2.8	[48]
UV_{254}: 0.25 mW·cm^{-2} H_2O_2: 10 mg·L^{-1} Time: 21.3 min Matrix: wastewater	*P. putida* MX-2 —	— *P. putida* MX-2 carried ARGs	5.25 0.7	— —	4.25 1.8	
UV_{254}: 3.46 mW·cm^{-2} H_2O_2: 5 mg·L^{-1} Time: 3 min Matrix: saline solution	*E. coli* and *P. aeruginosa*	—	—	—	~3.5	[65]
UV_{254}: 3.46 mW·cm^{-2} H_2O_2: 5 mg·L^{-1} Time: 8 min Matrix: wastewater	*E. coli* and *P. aeruginosa*	—	—	—	~3.5	
UV_{254}: 3.46 mW·cm^{-2} H_2O_2: 5 mg·L^{-1} Time: 90 min Matrix: wastewater	—	*sul1*, *sul2*, *tetM*, *blaOXA-A*, and *blaTEM*	—	—	2.0–3.7	
$UV_{320–450}$:— H_2O_2: 17 mg·L^{-1} Time: 45 min Matrix: surface water	*E. coli*	—	~1.5	< 0.1	6	[68]
$UV_{320–450}$: 17.4 μW·cm^{-2} H_2O_2: 20 mg·L^{-1} Time: 90 min Matrix: wastewater	*E. coli*	—	—	—	1.15	[66]
$UV_{320–450}$: 17.4 μW·cm^{-2} H_2O_2: 20 mg·L^{-1} Time: 240 min Matrix: wastewater	— —	*qnrS* and *blaTEM* *tetW*	— —	— —	< 0.1 0.74	
UV_{254}: 9.85 mW·cm^{-2} H_2O_2: 340 mg·L^{-1} Time: 30 min Matrix: wastewater	—	*sul1*, *tetX*, *tetG*, and *intI1*	—	—	1.55–2.32	[64]
UV_{254}: 100 mJ·cm^{-2} H_2O_2: 40 mg·L^{-1} Matrix: wastewater	Fecal coliforms	—	—	—	3.4	[69]
UV_{254}: 700 mJ·cm^{-2} H_2O_2: 40 mg·L^{-1} Matrix: wastewater	—	*blaOXA*, *blaTEM*, *blaCTX-M*, *qnrS*, *sul1*, and *tetM*	—	—	0.7–2.0	
UV_{254}: 2.3 μW·cm^{-2} H_2O_2: 34 mg·L^{-1} Time: 3 min Matrix: wastewater	*Klebsiella pneumoniae* (*K. pneumoniae*)	—	6	—	6	[45]
UV_{254}: 2.3 μW·cm^{-2} H_2O_2: 34 mg·L^{-1} Time: 5 min Matrix: wastewater	—	*blaKPC-3*	0.89	—	1.70	

(*continued on next page*)

Table 3 (*continued*)

Treatment	Target ARB	Target ARG	Reduction of ARB/ARGs (log)			Reference
			UV	H_2O_2	UV/H_2O_2	
UV_{254}: 0.55 mW·cm^{-2} H_2O_2: 10 mg·L^{-1} Time: 3 min Matrix: wastewater	*E. coli* PI7	—	5	—	6.2	[62]
	K. pneumonia L7	—	4.8	—	5.1	
UV_{254}: 0.55 mW·cm^{-2} H_2O_2: 10 mg·L^{-1} Time: 18 min Matrix: wastewater	—	*blaCTX-M-15*	2.7	—	2.7	
	—	*blaNDM-1*	2.1	—	2.9	

Table 4
Performance of UV, persulfate oxidation, and the combined UV/persulfate treatment in ARB inactivation and ARG degradation.

Treatment	Target ARB	Target ARG	Reduction of ARB/ARGs (log)			Reference
			UV	Persulfate	UV/persulfate	
UV_{254}: 0.1 mW·cm^{-2} PMS: 1 mg·L^{-1} Time: 10 min Matrix: PBS	*Pseudomonas* sp. HLS-6	—	4.1	0.28	5.3	[42]
UV_{254}: 0.1 mW·cm^{-2} PMS: 20 mg·L^{-1} Time: 30 min Matrix: PBS	—	*sul1*	1.2	2.0	2.9	
	—	*intI1*	0.7	2.3	3.4	
UV_{254}: 0.2 mW·cm^{-2} PMS: 5 mg·L^{-1} Time: 5 min Matrix: PBS	*Acinetobacter* sp. CS-2	—	7	4.7	7	[72]
UV_{254}: 0.2 mW·cm^{-2} PMS: 20 mg·L^{-1} Time: 30 min Matrix: PBS	—	*blaNDM-1*	1.63	~3.0	3.64	
	—	*blaOXA-58*	2.41	3.52	~4.6	
UV_{254}: 0.25 mW·cm^{-2} PDS: 45.6 mg·L^{-1} Time: 21.3 min Matrix: PBS	*P. putida* MX-2	—	6.97	—	6.97	[48]
	—	*P. putida* MX-2 carried ARGs	5.25	—	4.01	
UV_{254}: 0.25 mW·cm^{-2} PDS: 45.6 mg·L^{-1} Time: 21.3 min Matrix: PBS	*P. putida* MX-2	—	—	—	> 2	
	—	*P. putida* MX-2 carried ARGs	0.7	—	2.2	
UV_{254}: 2.3 μW·cm^{-2} PDS: 238 mg·L^{-1} Time: 3 min Matrix: wastewater	*K. pneumoniae*	—	6	—	6	[45]
UV_{254}: 2.3 μW·cm^{-2} PDS: 238 mg·L^{-1} Time: 5 min Matrix: wastewater	—	*blaKPC-3*	0.89	—	1.70	
UV_{254}: 45 μW·cm^{-2} PDS: 476 mg·L^{-1} or PMS: 304 mg·L^{-1} Time: 80 min Matrix: wastewater	*E. coli* J53	—	6.54	—	6.7 (UV/PDS), 6.58 (UV/ PMS)	[47]
UV_{254}: 4.5 μW·cm^{-2} PDS: 10 mg·L^{-1} Time: 30 min Matrix: wastewater	*E. coli*	—	4	—	6	[71]
UV_{254}: 0.01 kJ·L^{-1} PMS: 152 mg·L^{-1} Time: 6 min Matrix: wastewater	*E. coli*, *Enterococcus* spp., *Pseudomonas* spp.	—	—	—	3.5–5.8	[73]
UV_{254}: 0.4 mW·cm^{-2} PDS: 238 mg·L^{-1} Time: 10 min Matrix: wastewater	Total culturable bacteria	—	0.87–2.00	0.40–1.90	1.28–3.00	[46]
	—	*sul1*, *sul2*, *ermB*, *tetO*, *qnrS*, *intI1*, and *intI2*	0.16–1.09	0.02–0.66	0.24–1.14	

insignificantly contributed to ARG degradation in the UV/chlorine process. Similar results were obtained in previous studies [41,82], which indicated that the minor contribution of ·OH to ARG degradation was because ·OH could be easily consumed by cell surface components and the intracellular matrix. However, in a sample with benzoic acid as the scavenger of both ·OH and RCS, the reduction of *tetM* and *blaTEM* abundances was comparable to that with nitrobenzene as a scavenger of ·OH only [57], indicat-

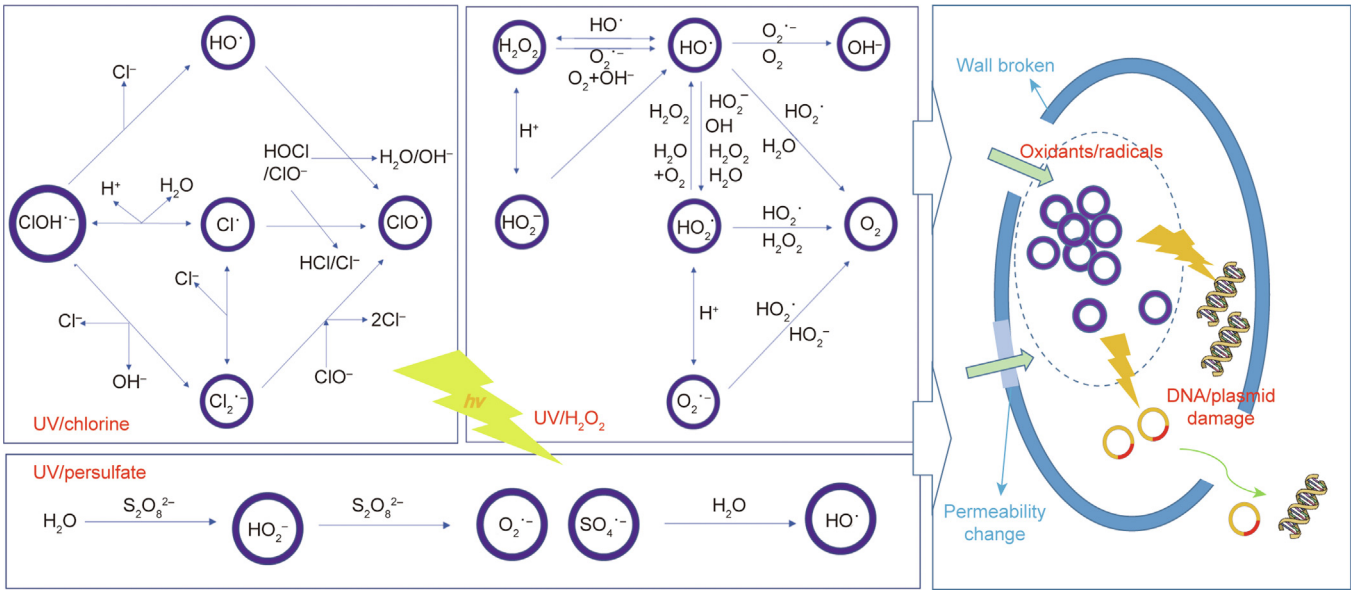

Fig. 2. Schematic illustration of radical formation, ARB inactivation, and ARG degradation in the UV/chlorine, UV/H_2O_2, and UV/persulfate processes [39,74]. hν indicates the photon energy; *h* is Plank's constant and ν is the frequency of the photon.

ing that ·OH instead of RCS primarily accounted for the *tetM* and *blaTEM* degradation in the UV/chlorine process. The inconsistency in the literature regarding the role of various radicals in ARG degradation could be ascribed to differences in bacterial strains and experimental conditions (e.g., UV and chlorine doses).

$$HOCl/OCl^- + h\nu \rightarrow HO^{\cdot}/O^{\cdot-} + Cl^{\cdot} \quad (1)$$

$$Cl^{\cdot} + Cl^- \leftrightarrow Cl_2^{\cdot-} \ (k_{+1} = 6.5 \times 10^9\ L \cdot mol^{-1} \cdot s^{-1},\ k_{-1} = 1.1 \times 10^5\ s^{-1}) \quad (2)$$

$$HOCl + HO^{\cdot} \rightarrow ClO^{\cdot} + H_2O \ (k = 2.0 \times 10^9\ L \cdot mol^{-1} \cdot s^{-1}) \quad (3)$$

$$OCl^- + HO^{\cdot} \rightarrow ClO^{\cdot} + OH^- \ (k = 8.8 \times 10^9\ L \cdot mol^{-1} \cdot s^{-1}) \quad (4)$$

$$HOCl + Cl^{\cdot} \rightarrow ClO^{\cdot} + H^+ + Cl^- \ (k = 3.0 \times 10^9\ L \cdot mol^{-1} \cdot s^{-1}) \quad (5)$$

$$OCl^- + Cl^{\cdot} \rightarrow ClO^{\cdot} + Cl^- \ (k = 8.2 \times 10^9\ L \cdot mol^{-1} \cdot s^{-1}) \quad (6)$$

In the UV/H_2O_2 process, ·OH is generated via the photolysis of H_2O_2 during the UV/H_2O_2 process, while a high concentration of H_2O_2 may serve as a ·OH scavenger, as shown in Eqs. (7)–(10) [67,83]. Due to the high reactivity and non-selectivity of ·OH, it is rapidly consumed by reactions with cell surface components, leading to its negligible impact on i-ARGs [41,63]. However, Meng et al. [48] observed a much greater degradation of i-ARGs with the UV/H_2O_2 process than with UV treatment alone. This might be because the permeability of the bacterial membrane can be altered by ·OH with increasing treatment time, allowing the penetration of UV irradiation and H_2O_2 into the cell and subsequent interactions with intracellular ARG-encoding DNA. In addition, it has been reported that the cytosol of bacteria can react with H_2O_2 to form ·OH, which can reduce enzyme activities, weaken metabolism, and cause mutagenic structural damage to DNA and RNA [45,84].

$$H_2O_2 + h\nu \rightarrow 2HO^{\cdot} \quad (7)$$

$$H_2O_2 + HO^{\cdot} \rightarrow HO_2^{\cdot} + H_2O \ (k = 2.7 \times 10^7\ L \cdot mol^{-1} \cdot s^{-1}) \quad (8)$$

$$HO^{\cdot} + HO_2^{\cdot} \rightarrow O_2 + H_2O \ (k = 6.6 \times 10^9\ L \cdot mol^{-1} \cdot s^{-1}) \quad (9)$$

$$HO^{\cdot} + HO^{\cdot} \rightarrow H_2O_2 \ (k = 5.5 \times 10^9\ L \cdot mol^{-1} \cdot s^{-1}) \quad (10)$$

The UV/PDS and UV/PMS processes are new AOPs that primarily produce ·OH and $SO_4^{\cdot-}$ (Fig. 2). The main chemical reactions involved are shown in Eqs. (11)–(15) at near neutral pH [85,86]. The quantum yields (Φ) of radicals from UV photolysis of PDS at 254 nm in deoxygenated (Φ = 1.4) and oxygen-saturated (Φ = 1.8) water are significantly higher than those of PMS (Φ = 1.04) and H_2O_2 (Φ = 1.0) [87]. Compared with ·OH, $SO_4^{\cdot-}$ has higher selectivity, a longer half-life (30–40 μs for $SO_4^{\cdot-}$ and 20 ns for ·OH), and a higher redox potential (2.5–3.1 V for $SO_4^{\cdot-}$ and 2.8 V for ·OH) [88]. Moreover, $SO_4^{\cdot-}$ can attack the guanine heterocycle at the π-site, resulting in DNA modification [42]. Accordingly, $SO_4^{\cdot-}$ has been reported to be the predominant reactive species responsible for inactivating ARB and degrading ARGs in the UV/PDS and UV/PMS processes [45]. However, the role of different radicals generated by UV/PDS or UV/PMS in bacterial inactivation and gene degradation may be influenced by bacterial strains and gene types. For instance, when tetracycline resistance genes in marine agricultural wastewater were treated with UV/PDS, $SO_4^{\cdot-}$ and ·OH mainly accounted for the degradation of *tetA* and *tetW*, respectively, and both radicals contributed significantly to the degradation of *tetM* [89].

$$S_2O_8^{2-} + h\nu \rightarrow 2SO_4^{\cdot-} \quad (11)$$

$$HSO_5^- + h\nu \rightarrow SO_4^{\cdot-} + HO^{\cdot} \quad (12)$$

$$SO_4^{\cdot-} + SO_4^{\cdot-} \rightarrow S_2O_8^{2-} \ (k = 4 \times 10^8\ L \cdot mol^{-1} \cdot s^{-1}) \quad (13)$$

$$SO_4^{\cdot-} + H_2O \rightarrow SO_4^{2-} + HO^{\cdot} + H^+ \ (k < 60\ L \cdot mol^{-1} \cdot s^{-1}) \quad (14)$$

$$SO_4^{\cdot-} + HO^{\cdot} \rightarrow HSO_5^- \ (k = 1 \times 10^{10}\ L \cdot mol^{-1} \cdot s^{-1}) \quad (15)$$

3. Factors influencing the efficiencies of the UV-based AOPs

3.1. Biotic factors

Extracellular polymeric substances (EPS) are organic polymers of microbial origin and include polysaccharides, proteins, extracellular DNA, and lipids [90]. As a fundamental component of biofilms, EPS can enhance the resistance of bacteria to

environmental stress. EPS acts as a shield that protects microbes from external damage, such as liquid shear force, antibiotics, and UV irradiation [48,91]. For UV-based AOPs, the dense EPS layer should be degraded first (e.g., by highly reactive radicals through oxidation of polysaccharides and proteins in EPS), and then UV irradiation, chemical oxidants, and free radicals can interact with the bacterial cells. Therefore, the treatment efficiencies of UV-based AOPs for ARB and ARGs are significantly affected by the EPS matrix. The treatment efficiencies are also related to bacterial type, as different bacteria have different resistances to external perturbation or destruction by UV, oxidants, and radicals. Jia et al. [92] observed that chlorination effectively reduced the levels of *Methylophilus*, *Methylotenera*, *Limnobacter*, and *Polynucleobacter*, while chlorination increased the relative abundance of *Pseudomonas*, *Acidovorax*, *Sphingomonas*, *Pleomonas*, and *Undibacterium* in drinking water. As UV fluence increased, the relative abundance of Gram-positive ARB in the microbial community increased [93]. This was attributed to the thicker peptidoglycan layers of Gram-positive ARB, which can inhibit UV penetration [93]. In addition, the smaller total genome size of Gram-positive ARB may reduce their susceptibility to UV irradiation because they have fewer latent pyrimidine dimers, the prominent targets of UV irradiation in DNA [94]. The initial levels of ARB could also impact treatment performance. A lower initial concentration of ARB may be associated with a higher inactivation efficiency [42] because the bacterial cytoplasm could release high concentrations of organics that consume radicals during UV-based AOP treatment. For the destruction of ARGs, the properties and structures of ARGs are crucial influencing factors. It has been reported that the efficiencies of UV and oxidants in degrading different types of genes are related to the target site, guanine content, and the number of latent dimers [42,95]. For instance, UV-induced ARG degradation was proportional to the number of adjacent thymine sites because UV irradiation causes DNA damage mainly through thymine dimerization [94].

3.2. Oxidant dose and UV fluence

Compared with ARB, the removal of ARGs by oxidants or UV irradiation usually requires much higher doses of UV and oxidants than those in conventional processes. However, the degradation of ARGs is not always proportional to the oxidant dose, as the overdosing of oxidants may cause a self-scavenging effect in radicals and an inner filter effect by competing for photons with target ARGs [38,42]. The optimal oxidant dose may vary for different target genes [44]. For instance, in the UV/chlorine process, the degradation of *sul1* gene increased as the chlorine dose was increased up to 5 $mg{\cdot}L^{-1}$, while no further enhancement was observed at higher chlorine doses; in contrast, the optimal chlorine dose for *intI1* gene removal was 20 $mg{\cdot}L^{-1}$ [44]. Zhang et al. [54] also reported that the synergism of ARG degradation increased significantly with chlorine dose from 15 to 25 $mg{\cdot}L^{-1}$ in the UV/chlorine process, whereas continuous increases in the chlorine dose resulted in an insignificant difference in ARG reduction. In the UV/H_2O_2 process, the maximum reduction of several commonly detected ARGs (e.g., *sul1*, *intI1*, *tetX*, and *tetG*) was achieved at an H_2O_2 dose of 340 $mg{\cdot}L^{-1}$ [64]; further increases in the H_2O_2 dose resulted in lower degradation efficiencies for the target ARGs, which was attributed to $^{\cdot}OH$ scavenging by higher concentrations of H_2O_2. Similarly, in the UV/PMS process, the optimal PMS dose for the degradation of *intI1* genes was 20 $mg{\cdot}L^{-1}$, while the degradation of *sul1* genes gradually increased up to a PMS dose of 30 $mg{\cdot}L^{-1}$ [42].

For UV-based AOPs, higher UV fluence can generally result in higher ARB inactivation and ARG reduction, and the fluence-based rate constants vary for different ARB and ARGs [60,62,63]. In particular, it was found that the degradation efficiency of *intI1* fluctuated with increasing UV fluence in the UV/PMS process [42], possibly due to its low sensitivity to direct UV photolysis. In addition to UV fluence, ARB inactivation efficiency may also be affected by UV wavelength [49,96]. Higher bacterial inactivation rates can be achieved by UV at 265 nm than UV at 254 nm [97]. For inactivating the bacteria *Campylobacter jejuni*, the combination of UV at 280 and 300 nm was demonstrated to show the best performance [98]. In studies focusing on UV-based AOPs, low-pressure UV (LPUV) lamps are most commonly used, primarily because approximately 82% of LPUV radiation is released at 254 nm (near the maximum UV absorption of nucleic acids at 260 nm) [99]. Medium-pressure UV (MPUV) lamps utilize mercury vapor with a UV radiation spectrum from 200 to 300 nm. An MPUV lamp requires higher electrical input (50–250 $W{\cdot}cm^{-1}$) and has a shorter lifetime (4000–8000 h) than an LPUV lamp (0.5–10 $W{\cdot}cm^{-1}$ and 8 000–10 000 h, respectively), while MPUV lamps are characterized by compact sizes and a wide range of applications [100]. Ultraviolet (UV) light-emitting diode (LED) is an emerging UV source. Although UV-LED has a relatively low wall-plug efficiency (typically less than 10%), its lack of mercury, variable wavelengths, and long lifetime make it an attractive alternative to conventional UV lamps [40,55,101]. Further studies on ARB and ARG control by UV-based AOPs using different UV sources are warranted.

3.3. pH

The pH of aquatic environments may vary greatly. While previous studies have described the insignificant effect of pH on ARB inactivation and ARG degradation by UV direct photolysis [41,102], pH plays a crucial role in the formation and transformation of reactive species and thus significantly affects the efficiency of UV-based AOPs. In general, acidic conditions are favorable for the control of ARB and ARGs by UV-based AOPs.

The UV/chlorine process usually performs better in acidic environments [44,103], mainly because of the species distribution of HOCl and OCl^- (pK_a = 7.5). Under acidic conditions, the dominant species of chlorine is HOCl, which has a higher quantum yield for radical generation and a lower radical scavenging capacity than OCl^- [104]. Additionally, HOCl is more effective than OCl^- in degrading ARGs due to its stronger oxidizing capacity [101]. When sample pH was increased from 5 to 9, a decreasing trend was observed for the reduction of *sul1* and *intI1* in the UV/chlorine treatment [44]. According to Eqs. (3)–(6), the scavenging of $^{\cdot}OH$ and $Cl^{\cdot}$ by HOCl was much slower than that by OCl^-, resulting in less degradation of *sul1* and *intI1* under alkaline conditions. For ARGs sensitive to $ClO^{\cdot}$, their degradation may increase with increasing pH. Yao et al. [105] reported a slight increase in the log reduction of *blaNDM-1* and *sul2* as pH increased from 6 to 8, mainly due to the elevated level of $ClO^{\cdot}$. The efficiency of the UV/H_2O_2 process for treating ARB and ARGs generally decreases with increasing pH value under water/wastewater treatment conditions [64,106]. For instance, the degradation of target ARGs (i.e., *sul1*, *intI1*, *tetX*, and *tetG*) during UV/H_2O_2 treatment of wastewater decreased as pH increased from 3.5 to 9.0 [64]. Under alkaline conditions, the formation of HO_2^- from H_2O_2/HO_2^- equilibrium (pK_a = 11.7) becomes significant [107]. The formed HO_2^- can further react with H_2O_2 (Eq. (16)), causing a decrease in the concentration of $^{\cdot}OH$. Moreover, the reaction rate constant of $^{\cdot}OH$ with HO_2^- is over 100 times higher than that with H_2O_2 (Eqs. (8) and (17)), indicating the enhanced scavenging of $^{\cdot}OH$ with increasing pH.

$$HO_2^- + H_2O_2 \rightarrow O_2 + H_2O + OH^- \quad (16)$$

$$HO_2^- + HO^{\cdot} \rightarrow HO_2^{\cdot} + OH^- (k = 7.5 \times 10^9\ L \cdot mol^{-1} \cdot s^{-1}) \quad (17)$$

In the UV/PDS or UV/PMS process, ARB inactivation has been reported to decrease with increasing pH in water or wastewater treatment [84,101], which is attributed to the enhanced

decomposition of PDS or PMS and the transformation of radical species [108]. Similarly, in the pH range of 5–9, a higher reduction of target ARGs (*sul1* and *intI1*) was achieved by the UV/PMS process under acidic conditions [42]. Under alkaline conditions, $SO_4^{\cdot-}$ formed from UV-activated PDS or PMS can react with OH^- to generate $^{\cdot}OH$ (Eq. (18)). The coexistence of $SO_4^{\cdot-}$ and $^{\cdot}OH$ may result in the rapid transformation of radicals to PMS, as shown in Eq. (15) [109], which negatively affects the performance of the UV/persulfate process. Meanwhile, in UV/PDS treatment of target ARGs (i.e., *blaTEM*, *qnrS*, *tetW*, and *tetE*) at pH values of 3.4, 7.3, and 11.1, less than 20% variation in ARG degradation was observed [110], which might be due to the comparable contributions of $SO_4^{\cdot-}$ and $^{\cdot}OH$ to the ARG degradation.

$$SO_4^{\cdot-} + OH^- \rightarrow HO^{\cdot} + SO_4^{2-} \ (k = 6.5 \times 10^7\ L \cdot mol^{-1} \cdot s^{-1}) \quad (18)$$

pH also affects the distributions of H_2CO_3/HCO_3^- (pK_a = 6.4) and HCO_3^-/CO_3^{2-} (pK_a = 10.3). $CO_3^{\cdot-}$ could be produced by the reaction of $^{\cdot}OH$, RCS, or $SO_4^{\cdot-}$ with HCO_3^- or CO_3^{2-} (Eqs. (19)–(21)) [103]. The concentration of $CO_3^{\cdot-}$ has been found to be much higher in the UV/chlorine process than in the UV/H_2O_2 process [104], which in turn is likely to be higher than that in the UV/persulfate process, due to the descending reaction rate constants of HCO_3^- with $Cl^{\cdot}$, $^{\cdot}OH$, and $SO_4^{\cdot-}$. With increasing pH, the proportion of HCO_3^- and CO_3^{2-} may also increase, which is unfavorable for ARB inactivation and ARG degradation because of the scavenging effect.

$$HCO_3^-/CO_3^{2-} + HO^{\cdot} \rightarrow CO_3^{\cdot-} + H_2O/OH^-$$
$$(k_{HCO_3^-} = 8.5 \times 10^6\ L \cdot mol^{-1} \cdot s^{-1},$$
$$k_{CO_3^{2-}} = 3.9 \times 10^8\ L \cdot mol^{-1} \cdot s^{-1}) \quad (19)$$

$$HCO_3^-/CO_3^{2-} + Cl^{\cdot} \rightarrow CO_3^{\cdot-} + HCl/Cl^-$$
$$(k_{HCO_3^-} = 2.2 \times 10^8\ L \cdot mol^{-1} \cdot s^{-1},$$
$$k_{CO_3^{2-}} = 5.0 \times 10^8\ L \cdot mol^{-1} \cdot s^{-1}) \quad (20)$$

$$HCO_3^-/CO_3^{2-} + SO_4^{\cdot-} \rightarrow CO_3^{\cdot-} + HSO_4^-/SO_4^{2-}$$
$$(k_{HCO_3^-} = 1.6 \times 10^6\ L \cdot mol^{-1} \cdot s^{-1},$$
$$k_{CO_3^{2-}} = 6.1 \times 10^6\ L \cdot mol^{-1} \cdot s^{-1}) \quad (21)$$

3.4. Water matrix

An increasing number of studies have focused on ARB inactivation and ARG degradation in real water/wastewater, where the water matrix (e.g., suspended solids, dissolved organic matter (DOM), inorganic anions, and metals) may significantly affect the efficiency of UV-based AOPs [71,111–113]. The negative effect of suspended solids on the efficiency of UV-based AOPs due to the shielding of ARB/ARGs from UV irradiation and chemical oxidation is well acknowledged. For example, the inactivation rate of carbapenem resistant *K. pneumoniae* by UV/PDS was three times higher in PBS than in secondary wastewater effluent [45]. In contrast, Yoon et al. [41] found that only slightly higher UV fluence was required for ARG degradation in filtered wastewater effluent (i.e., without suspended solids) compared with that in PBS. While DOM in the water matrix is a major consumer of free radicals, it shows limited consumption of chemical oxidants and UV irradiation [49,103]. It has been reported that ARG degradation by UV/H_2O_2 and UV/PDS processes was inhibited in the presence of DOM compared with the conditions without DOM [63,95], which was due to radical scavenging by DOM. A significant decrease in radicals was observed in the UV/chlorine process in the presence of 5 mg·L^{-1} DOM, with reductions in the concentrations of $Cl^{\cdot}$, $^{\cdot}OH$, and $ClO^{\cdot}$ by 18%, 27%, and 99%, respectively [103]. Interestingly, when only UV irradiation was used, the presence of DOM could even enhance the degradation of ARGs, which was ascribed to the generation of reactive species via the UV photolysis of DOM [63,95].

The presence of inorganic anions (e.g., Cl^-, Br^-, and SO_4^{2-}) in the water matrix may affect the performance of UV-based AOPs by radical scavenging [104]. For ARB/ARGs that are not susceptible to radicals, inorganic anions have shown insignificant inhibition in their removal [72,105]. The presence of chloride in a PMS treatment system was found to enhance the inactivation of *E. coli* and *Bacillus* spores due to the formation of HOCl/OCl^- from the reaction of PMS with Cl^- [114]. Studies [111,115] have reported positive correlations of metals (e.g., Ag(I), Cu(II), Hg(II), Zn(II), and Cr(VI)) with ARG levels in aquatic environments due to the co-selection of ARGs by metals and the promotion of horizontal gene transfer at subinhibitory concentrations of metals. For instance, Cu(II) at environmentally relevant concentrations (1–100 μmol·L^{-1}) could increase conjugation frequencies of plasmid-encoded ARGs by increasing cell membrane permeability and altering conjugative regulators [112]. In UV-based AOPs, the presence of metals with multiple redox states (e.g., Cu(I)/Cu(II), Fe(II)/Fe(III), and Mn(II)/Mn(IV)) could catalyze the decomposition of H_2O_2 and persulfate and enable the production of $^{\cdot}OH$ and $SO_4^{\cdot-}$, respectively, by Fenton and Fenton-like reactions [116,117]. The reactions of copper with H_2O_2, PDS, or PMS in the UV systems are described in Eqs. (22)–(25). In the Fe(II)-containing system, Fe(IV) could form and also contribute to lipid peroxidation and DNA damage [113].

$$Cu^{2+} + h\nu \rightarrow Cu^+ \quad (22)$$

$$Cu^+ + H_2O_2 \rightarrow HO^{\cdot} + OH^- + Cu^{2+} \quad (23)$$

$$Cu^+ + S_2O_8^{2-} \rightarrow SO_4^{\cdot-} + SO_4^{2-} + Cu^{2+} \quad (24)$$

$$Cu^+ + HSO_5^- \rightarrow SO_4^{\cdot-} + OH^- + Cu^{2+} \quad (25)$$

4. Analysis of cost-effectiveness of the UV-based AOPs

One of the most critical factors that impact the application of a new technology is cost, which includes capital and operating costs. The capital costs of UV-based AOPs have been reported to be lower than those of other advanced technologies, such as ozonation and membrane technologies (e.g., reverse osmosis) [118]. To further evaluate the cost-effectiveness of the UV-based AOPs discussed in this study, their operating costs (including energy consumption and chemical oxidant costs) for ARB/ARG treatment were evaluated. The operating costs could be roughly estimated by the EE/O (i.e., the electrical energy required to reduce ARB/ARG levels in one cubic meter of a water sample by one order of magnitude (kW·h·m^{-3}·$order^{-1}$)) [109,119], consisting of electrical energy for the UV source (EE/O_{UV}) and equivalent electrical energy for the consumption of oxidants ($EE/O_{oxidant}$). The EE/O values can be calculated using Eqs. (26)–(28):

$$EE/O = EE/O_{UV} + EE/O_{oxidant} \quad (26)$$

$$EE/O_{UV} = \frac{A \times I \times t}{1000 \times E \times V \times \log\frac{C_0}{C_t}} \quad (27)$$

$$EE/O_{oxidant} = Eq_{oxidant} \times \frac{D_{oxidant} \times 1000}{\log\frac{C_0}{C_t}} \quad (28)$$

where A is the irradiated surface area (cm^2), I is the UV fluence rate (mW·cm^{-2}), t is the reaction time (h), V is the volume of the treated water samples (L), and E is the wall-plug efficiency.

Since LPUV is the most commonly used UV source in studies on ARB and ARG treatment with UV-based AOPs, an E value of 0.32 was adopted according to Wan et al. [120]. C_0 and C_t are the initial and final concentrations of the selected ARGs, respectively. $Eq_{oxidant}$ represents the electrical energy consumption required to generate one mole of an oxidant (kW·h·mol^{-1}), and $D_{oxidant}$ represents the dose of the oxidant (mol·L^{-1}). Using the average electricity cost (approximately 0.193 USD·(kW·h)$^{-1}$ [121] and chemical prices from manufacturers and suppliers on a well-known e-commerce platform[†], we calculated the $Eq_{oxidant}$ values for chlorine, H_2O_2, PDS, and PMS to be 4.64, 3.44, 4.98, and 7.79 kW·h·mol^{-1}, respectively. Using the UV fluences and chemical doses reported in previous studies for ARB/ARG treatment (Tables 2–4), we determined the costs for energy consumption and chemical oxidants in different UV-based AOPs.

Fig. 3 shows the EE/O_{UV} and $EE/O_{oxidant}$ of different UV-based AOPs for ARB/ARG treatment in PBS or wastewater. A higher EE/O is indicative of a low energy efficiency of the corresponding treatment [119]. The median EE/O values of UV/chlorine, UV/H_2O_2, and UV/persulfate processes for ARG degradation in PBS and wastewater were averagely 7.7 and 29.7 times larger than those for ARB inactivation, respectively. This indicates that, compared with ARG degradation, UV-based AOPs are generally very effective in ARB inactivation. In the PBS solution, the UV/persulfate process was the most cost-effective UV-based AOP (Fig. 3(a)). Both the median values of EE/O_{UV} and $EE/O_{oxidant}$ in the UV/persulfate process for ARG degradation (0.064 and 0.324 kW·h·m^{-3}·order^{-1}, respectively) were lower than the corresponding values in UV/chlorine (0.334 and 0.408 kW·h·m^{-3}·order^{-1}, respectively) and UV/H_2O_2 (0.266 and 1.720 kW·h·m^{-3}·order^{-1}, respectively) processes. In the PBS solution without interferences from the water matrix, the relatively high $EE/O_{oxidant}$ of the UV/H_2O_2 process might be attributed to the lower absorbance coefficients of H_2O_2 (18.6 mol^{-1}·cm^{-1}) than those of other oxidants (e.g., 59 mol^{-1}·cm^{-1} for HOCl and 27.5 mol^{-1}·cm^{-1} for PDS) at UV 254 nm [55,122]. The UV/H_2O_2 process usually requires excess H_2O_2 because only 5%–10% of the dosed H_2O_2 is consumed by UV photolysis, which leads to an increase in chemical costs [122]. Additional chemicals are required to remove the remaining H_2O_2; accordingly, the operation of the UV/H_2O_2 process is relatively complex and less effective in terms of energy utilization [123]. However, in a wastewater matrix, the UV/chlorine process showed higher energy efficiency than other UV-based AOPs (Fig. 3(b)). Although the median EE/O_{UV} of the UV/persulfate process for ARG degradation (0.179 kW·h·m^{-3}·order^{-1}) was lower than that of the UV/chlorine and UV/H_2O_2 processes (0.421 and 0.277 kW·h·m^{-3}·order^{-1}, respectively), the median $EE/O_{oxidant}$ increased significantly to 9.68 kW·h·m^{-3}·order^{-1}. The higher energy efficiency of UV/chlorine in wastewater might result from the higher disinfection efficacy of chlorine than H_2O_2 and persulfate [76,77] and the comparatively high selectivity of RCS over $^{\cdot}OH$ and $SO_4^{\cdot-}$ [124]. Similar results have been reported for cost-effectiveness analysis related to the removal of emerging contaminants in wastewater [118,125]. Guo et al. [119] reported that the electrical energy required for organic pollutant removal was lower in the UV/chlorine process than in the UV/H_2O_2 process. With regard to emerging contaminant degradation, the UV/chlorine process resulted in savings of 30%–75% in electrical energy compared with the UV/H_2O_2 process, resulting in a remarkable 30%–50% reduction in operating costs and a potential reduction in capital costs owing to the smaller number of reactor chambers required for the UV/chlorine process [118]. A previous review [126] summarized the energy efficiency-of UV-based AOPs in the degradation of pharmaceuticals and indicated that the EE/O values followed the order of $EE/O_{UV/catalyst}$ > $EE/O_{UV/H_2O_2}$ > $EE/O_{UV/persulfate}$ > $EE/O_{UV/chlorine}$.

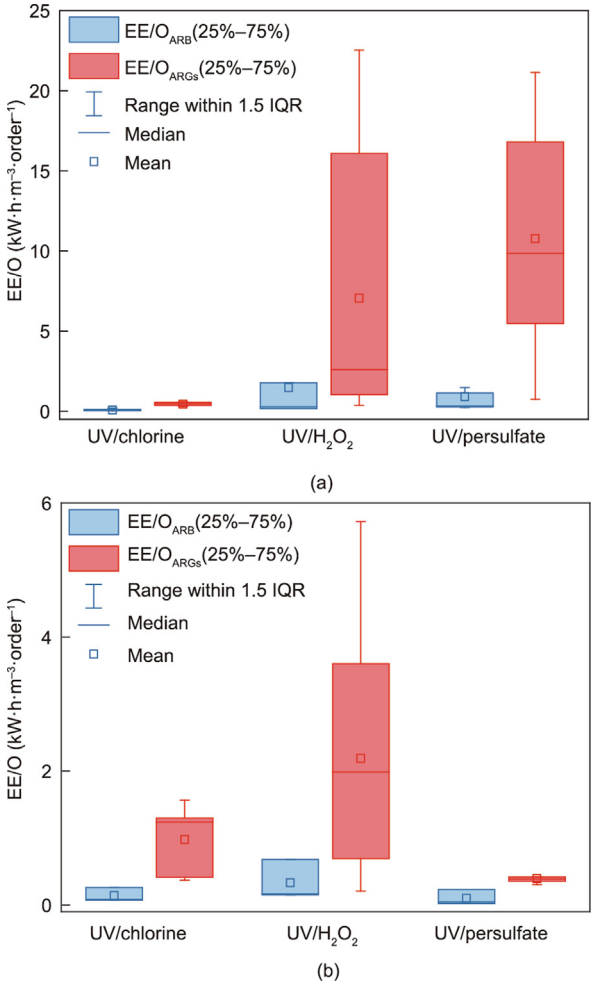

Fig. 3. EE/O of the UV/chlorine, UV/H_2O_2, and UV/persulfate processes for controlling ARB and ARGs in (a) PBS and (b) wastewater samples. IQR indicates interquartile range.

It is worth noting that in the EE/O analysis, the number of available data (n) for the UV/chlorine (n = 9) and UV/persulfate (n = 13) processes was smaller than that for the UV/H_2O_2 process (n = 27), possibly because UV/chlorine and UV/persulfate are new AOPs. More studies on ARG degradation by different UV-based AOPs are thus warranted to further improve the EE/O analysis. Additionally, despite the cost-effectiveness of the UV/chlorine process in treating ARB and ARGs, halogenated disinfection byproducts (DBPs) can be readily formed from reactions of DOM with chlorine and RCS in this process [104,127,128]. UV/chlorine treatment of drinking water and wastewater has been reported to generate more halogenated DBPs than chlorination alone [128,129]. As many halogenated DBPs are cytotoxic, genotoxic, and developmentally toxic [130–135], increased toxicity of wastewater effluent from UV/chlorine treatment has been observed [136] as a consequence of DBP formation. Concerns about the formation of toxic halogenated byproducts should be thoroughly evaluated before the application of the UV/chlorine process.

5. Conclusions and prospects

UV-based AOPs (e.g., UV/chlorine, UV/H_2O_2, and UV/persulfate) are considered promising control technologies to address the pressing health concerns associated with ARB and ARGs. Due to

[†] https://www.alibaba.com/.

the generation of multiple reactive species, these integrated AOP systems show significantly higher treatment efficiencies than direct UV photolysis or chemical oxidation alone. However, the specific reactive species mainly responsible for ARB inactivation and ARG degradation depend on the target bacterial strains and gene types. The efficiency of UV-based AOPs can be influenced by factors such as types and conditions of target ARB and ARGs, chemical dose and UV fluence, pH, and water matrix properties. The combined effects of these influencing factors further complicate the control of ARB and ARGs by UV-based AOPs. To evaluate the feasibility of using UV-based AOPs for ARB and ARG control, the EE/O values (considering the electrical energy for LPUV lamps and chemical oxidants) of the UV/chlorine, UV/H_2O_2, and UV/persulfate processes were analyzed. According to the EE/O results, while the UV/persulfate process showed the best energy efficiency in PBS solution, the UV/chlorine process was most efficient in real wastewater. The different EE/O rank orders highlighted the influence of the water matrix on the efficiency of UV-based AOPs. Additionally, the type of UV lamps used (e.g., LPUV versus MPUV and UV-LED) and the treatment capacity (e.g., laboratory-scale versus pilot- and full-scale) may also affect the cost evaluation for different UV-based AOPs, necessitating further investigation and systematic assessment. Notably, although the UV/chlorine process was more cost-effective in controlling ARB and ARGs than other UV-based AOPs, the formation of toxic byproducts during the UV/chlorine process may counteract its benefits and should be carefully evaluated.

Acknowledgments

The work described in this paper was supported by grants from the Research Grants Council of the Hong Kong SAR, China (T21-705/20-N and 16210221).

Compliance with ethics guidelines

Jiarui Han, Wanxin Li, Yun Yang, Xuanwei Zhang, Siyu Bao, Xiangru Zhang, Tong Zhang, and Kenneth Mei Yee Leung declare that they have no conflict of interest or financial conflicts to disclose.

References

[1] Travis A, Chernova O, Chernov V, Aminov R. Antimicrobial drug discovery: lessons of history and future strategies. Expert Opin Drug Discov 2018;13(11):983–5.
[2] Kümmerer K. Antibiotics in the aquatic environment—a review—part I. Chemosphere 2009;75(4):417–34.
[3] Klein EY, Van Boeckel TP, Martinez EM, Pant S, Gandra S, Levin SA, et al. Global increase and geographic convergence in antibiotic consumption between 2000 and 2015. Proc Natl Acad Sci USA 2018;115(15):E3463–70.
[4] Zhang Z, Zhang Q, Wang T, Xu N, Lu T, Hong W, et al. Assessment of global health risk of antibiotic resistance genes. Nat Commun 2022;13(1):1553.
[5] Rodriguez-Mozaz S, Chamorro S, Marti E, Huerta B, Gros M, Sànchez-Melsió A, et al. Occurrence of antibiotics and antibiotic resistance genes in hospital and urban wastewaters and their impact on the receiving river. Water Res 2015;69:234–42.
[6] Yang C, Wang L, Wang H, Zhang H, Wang F, Zhou H, et al. Dynamics of antibiotic resistance genes and microbial community in shortcut nitrification–denitrification process under antibiotic stresses. Environ Sci Pollut Res Int 2022;29(31):46848–58.
[7] Dadgostar P. Antimicrobial resistance: implications and costs. Infect Drug Resist 2019;12:3903–10.
[8] Qu S, Huang X, Song X, Wu Y, Ma X, Shen J, et al. A rigid nanoplatform for precise and responsive treatment of intracellular multidrug-resistant bacteria. Engineering 2022;15:57–66.
[9] Murray CJL, Ikuta KS, Sharara F, Swetschinski L, Robles Aguilar G, Gray A, et al. Global burden of bacterial antimicrobial resistance in 2019: a systematic analysis. Lancet 2022;399(10325):629–55.
[10] Von Wintersdorff CJH, Penders J, van Niekerk JM, Mills ND, Majumder S, van Alphen LB, et al. Dissemination of antimicrobial resistance in microbial ecosystems through horizontal gene transfer. Front Microbiol 2016;7:173.
[11] Tenover FC. Mechanisms of antimicrobial resistance in bacteria. Am J Med 2006;119(6):S3–10.
[12] Shi X, Xia Y, Wei W, Ni BJ. Accelerated spread of antibiotic resistance genes (ARGs) induced by non-antibiotic conditions: roles and mechanisms. Water Res 2022;224:119060.
[13] Dodd MC. Potential impacts of disinfection processes on elimination and deactivation of antibiotic resistance genes during water and wastewater treatment. J Environ Monit 2012;14(7):1754–71.
[14] Sui Q, Chen Y, Yu D, Wang T, Hai Y, Zhang J, et al. Fates of intracellular and extracellular antibiotic resistance genes and microbial community structures in typical swine wastewater treatment processes. Environ Int 2019;133:105183.
[15] Vikesland PJ, Pruden A, Alvarez PJJ, Aga D, Bürgmann H, Li XD, et al. Toward a comprehensive strategy to mitigate dissemination of environmental sources of antibiotic resistance. Environ Sci Technol 2017;51(22):13061–9.
[16] Dong P, Wang H, Fang T, Wang Y, Ye Q. Assessment of extracellular antibiotic resistance genes (eARGs) in typical environmental samples and the transforming ability of eARG. Environ Int 2019;125:90–6.
[17] Calero-Cáceres W, Ye M, Balcázar JL. Bacteriophages as environmental reservoirs of antibiotic resistance. Trends Microbiol 2019;27(7):570–7.
[18] Marti E, Variatza E, Balcazar JL. The role of aquatic ecosystems as reservoirs of antibiotic resistance. Trends Microbiol 2014;22(1):36–41.
[19] Bougnom BP, Piddock LJV. Wastewater for urban agriculture: a significant factor in dissemination of antibiotic resistance. Environ Sci Technol 2017;51(11):5863–4.
[20] Rowe WPM, Baker-Austin C, Verner-Jeffreys DW, Ryan JJ, Micallef C, Maskell DJ, et al. Overexpression of antibiotic resistance genes in hospital effluents over time. J Antimicrob Chemother 2017;72(6):1617–23.
[21] Sousa JCG, Ribeiro AR, Barbosa MO, Pereira MFR, Silva AMT. A review on environmental monitoring of water organic pollutants identified by EU guidelines. J Hazard Mater 2018;344:146–62.
[22] Krzeminski P, Tomei MC, Karaolia P, Langenhoff A, Almeida CMR, Felis E, et al. Performance of secondary wastewater treatment methods for the removal of contaminants of emerging concern implicated in crop uptake and antibiotic resistance spread: a review. Sci Total Environ 2019;648:1052–81.
[23] Cizmas L, Sharma VK, Gray CM, McDonald TJ. Pharmaceuticals and personal care products in waters: occurrence, toxicity, and risk. Environ Chem Lett 2015;13(4):381–94.
[24] Lee J, Jeon JH, Shin J, Jang HM, Kim S, Song MS, et al. Quantitative and qualitative changes in antibiotic resistance genes after passing through treatment processes in municipal wastewater treatment plants. Sci Total Environ 2017;605–606:906–14.
[25] Reichert G, Hilgert S, Alexander J, Rodrigues de Azevedo JC, Morck T, Fuchs S, et al. Determination of antibiotic resistance genes in a WWTP-impacted river in surface water, sediment, and biofilm: influence of seasonality and water quality. Sci Total Environ 2021;768.
[26] Wilkinson JL, Boxall ABA, Kolpin DW, Leung KMY, Lai RWS, Galbán-Malagón C, et al. Pharmaceutical pollution of the world's rivers. Proc Natl Acad Sci USA 2022;119(8):e2113947119.
[27] Uluseker C, Kaster KM, Thorsen K, Basiry D, Shobana S, Jain M, et al. A review on occurrence and spread of antibiotic resistance in wastewaters and in wastewater treatment plants: mechanisms and perspectives. Front Microbiol 2021;12:717809.
[28] Li S, Ondon BS, Ho SH, Zhou Q, Li F. Drinking water sources as hotspots of antibiotic-resistant bacteria (ARB) and antibiotic resistance genes (ARGs): occurrence, spread, and mitigation strategies. J Water Process Eng 2023;53:103907.
[29] Su HC, Liu YS, Pan CG, Chen J, He LY, Ying GG. Persistence of antibiotic resistance genes and bacterial community changes in drinking water treatment system: from drinking water source to tap water. Sci Total Environ 2018;616–617:453–61.
[30] Mackenzie D. Ultraviolet light fights new virus. Engineering 2020;6(8):851–3.
[31] Sharma VK, Yu X, McDonald TJ, Jinadatha C, Dionysiou DD, Feng M. Elimination of antibiotic resistance genes and control of horizontal transfer risk by UV-based treatment of drinking water: a mini review. Front Environ Sci Eng 2019;13(3):37.
[32] Hu Q, Zhang XX, Jia S, Huang K, Tang J, Shi P, et al. Metagenomic insights into ultraviolet disinfection effects on antibiotic resistome in biologically treated wastewater. Water Res 2016;101:309–17.
[33] Liu SS, Qu HM, Yang D, Hu H, Liu WL, Qiu ZG, et al. Chlorine disinfection increases both intracellular and extracellular antibiotic resistance genes in a full-scale wastewater treatment plant. Water Res 2018;136:131–6.
[34] Yuan Q, Yu P, Cheng Y, Zuo P, Xu Y, Cui Y, et al. Chlorination (but not UV disinfection) generates cell debris that increases extracellular antibiotic resistance gene transfer via proximal adsorption to recipients and upregulated transformation genes. Environ Sci Technol 2022;56(23):17166–76.
[35] Liu H, Li Z, Liu C, Qiang Z, Karanfil T, Yang M. Elimination and redistribution of intracellular and extracellular antibiotic resistance genes in water and wastewater disinfection processes: a review. ACS EST Water 2022;2(12):2273–88.
[36] Hu Y, Zhang T, Jiang L, Luo Y, Yao S, Zhang D, et al. Occurrence and reduction of antibiotic resistance genes in conventional and advanced drinking water treatment processes. Sci Total Environ 2019;669:777–84.
[37] Guo MT, Kong C. Antibiotic resistant bacteria survived from UV disinfection: safety concerns on genes dissemination. Chemosphere 2019;224:827–32.

[38] Zhang G, Li W, Chen S, Zhou W, Chen J. Problems of conventional disinfection and new sterilization methods for antibiotic resistance control. Chemosphere 2020;254:126831.
[39] Gmurek M, Borowska E, Schwartz T, Horn H. Does light-based tertiary treatment prevent the spread of antibiotic resistance genes? Performance, regrowth and future direction. Sci Total Environ 2022;817:153001.
[40] Zhang Y, Zhao YG, Maqbool F, Hu Y. Removal of antibiotics pollutants in wastewater by UV-based advanced oxidation processes: influence of water matrix components, processes optimization and application: a review. J Water Process Eng 2022;45:102496.
[41] Yoon Y, Chung HJ, Wen Di DY, Dodd MC, Hur HG, Lee Y. Inactivation efficiency of plasmid-encoded antibiotic resistance genes during water treatment with chlorine, UV, and UV/H_2O_2. Water Res 2017;123:783–93.
[42] Hu Y, Zhang T, Jiang L, Yao S, Ye H, Lin K, et al. Removal of sulfonamide antibiotic resistant bacterial and intracellular antibiotic resistance genes by UVC-activated peroxymonosulfate. Chem Eng J 2019;368:888–95.
[43] Lee H, Lee E, Lee CH, Lee K. Degradation of chlorotetracycline and bacterial disinfection in livestock wastewater by ozone-based advanced oxidation. J Ind Eng Chem 2011;17(3):468–73.
[44] Zhang T, Hu Y, Jiang L, Yao S, Lin K, Zhou Y, et al. Removal of antibiotic resistance genes and control of horizontal transfer risk by UV, chlorination and UV/chlorination treatments of drinking water. Chem Eng J 2019;358:589–97.
[45] Serna-Galvis EA, Salazar-Ospina L, Jiménez JN, Pino NJ, Torres-Palma RA. Elimination of carbapenem resistant *Klebsiella pneumoniae* in water by UV-C, UV-C/persulfate and UV-C/H_2O_2. Evaluation of response to antibiotic, residual effect of the processes and removal of resistance gene. J Environ Chem Eng 2020;8(1):102196.
[46] Zhou C, Wu J, Dong L, Liu B, Xing D, Yang S, et al. Removal of antibiotic resistant bacteria and antibiotic resistance genes in wastewater effluent by UV-activated persulfate. J Hazard Mater 2020;388:122070.
[47] Arslan-Alaton I, Karatas A, Pehlivan Ö, Koba Ucun O, Ölmez-Hancı T. Effect of UV-A-assisted iron-based and UV-C-driven oxidation processes on organic matter and antibiotic resistance removal in tertiary treated urban wastewater. Catal Today 2021;361:152–8.
[48] Meng X, Li F, Yi L, Dieketseng MY, Wang X, Zhou L, et al. Free radicals removing extracellular polymeric substances to enhance the degradation of intracellular antibiotic resistance genes in multi-resistant *Pseudomonas Putida* by UV/H_2O_2 and UV/peroxydisulfate disinfection processes. J Hazard Mater 2022;430:128502.
[49] Umar M, Roddick F, Fan L. Moving from the traditional paradigm of pathogen inactivation to controlling antibiotic resistance in water—role of ultraviolet irradiation. Sci Total Environ 2019;662:923–39.
[50] Zhong J, Yang B, Gao FZ, Xiong Q, Feng Y, Li Y, et al. Performance and mechanism in degradation of typical antibiotics and antibiotic resistance genes by magnetic resin-mediated UV-Fenton process. Ecotoxicol Environ Saf 2021;227:112908.
[51] Chen X, Han W, Patel M, Wang Q, Li Q, Zhao S, et al. Inactivation of a pathogenic NDM-1-positive *Escherichia coli* strain and the resistance gene *bla*NDM-1 by TiO_2/UVA photocatalysis. Sci Total Environ 2022;846:157369.
[52] Jäger T, Hembach N, Elpers C, Wieland A, Alexander J, Hiller C, et al. Reduction of antibiotic resistant bacteria during conventional and advanced wastewater treatment, and the disseminated loads released to the environment. Front Microbiol 2018;9:2599.
[53] Xue W, Zhang C, Zhou D. Positive and negative effects of recirculating aquaculture water advanced oxidation: O_3 and O_3/UV treatments improved water quality but increased antibiotic resistance genes. Water Res 2023;235:119835.
[54] Zhang Y, Zhuang Y, Geng J, Ren H, Zhang Y, Ding L, et al. Inactivation of antibiotic resistance genes in municipal wastewater effluent by chlorination and sequential UV/chlorination disinfection. Sci Total Environ 2015;512–513:125–32.
[55] Miklos DB, Remy C, Jekel M, Linden KG, Drewes JE, Hübner U. Evaluation of advanced oxidation processes for water and wastewater treatment—a critical review. Water Res 2018;139:118–31.
[56] Liu X, Hu J. Effect of DNA sizes and reactive oxygen species on degradation of sulphonamide resistance *sul1* genes by combined UV/free chlorine processes. J Hazard Mater 2020;392:122283.
[57] Phattarapattamawong S, Chareewan N, Polprasert C. Comparative removal of two antibiotic resistant bacteria and genes by the simultaneous use of chlorine and UV irradiation (UV/chlorine): influence of free radicals on gene degradation. Sci Total Environ 2021;755:142696.
[58] Ye C, Chen Y, Feng L, Wan K, Li J, Feng M, et al. Effect of the ultraviolet/chlorine process on microbial community structure, typical pathogens, and antibiotic resistance genes in reclaimed water. Front Environ Sci Eng 2022;16(8):100.
[59] Shekhawat SS, Kulshreshtha NM, Vivekanand V, Gupta AB. Impact of combined chlorine and UV technology on the bacterial diversity, antibiotic resistance genes and disinfection by-products in treated sewage. Bioresour Technol 2021;339:125615.
[60] Wang H, Wang J, Li S, Ding G, Wang K, Zhuang T, et al. Synergistic effect of UV/chlorine in bacterial inactivation, resistance gene removal, and gene conjugative transfer blocking. Water Res 2020;185:116290.
[61] Zeng F, Cao S, Jin W, Zhou X, Ding W, Tu R, et al. Inactivation of chlorine-resistant bacterial spores in drinking water using UV irradiation, UV/hydrogen peroxide and UV/peroxymonosulfate: efficiency and mechanism. J Clean Prod 2020;243:118666.
[62] Augsburger N, Zaouri N, Cheng H, Hong PY. The use of UV/H_2O_2 to facilitate removal of emerging contaminants in anaerobic membrane bioreactor effluents. Environ Res 2021;198:110479.
[63] Das D, Bordoloi A, Achary MP, Caldwell DJ, Suri RPS. Degradation and inactivation of chromosomal and plasmid encoded resistance genes/ARBs and the impact of different matrices on UV and UV/H_2O_2 based advanced oxidation process. Sci Total Environ 2022;833:155205.
[64] Zhang Y, Zhuang Y, Geng J, Ren H, Xu K, Ding L. Reduction of antibiotic resistance genes in municipal wastewater effluent by advanced oxidation processes. Sci Total Environ 2016;550:184–91.
[65] Michael SG, Michael-Kordatou I, Nahim-Granados S, Polo-López MI, Rocha J, Martínez-Piernas AB, et al. Investigating the impact of UV-C/H_2O_2 and sunlight/H_2O_2 on the removal of antibiotics, antibiotic resistance determinants and toxicity present in urban wastewater. Chem Eng J 2020;388:124383.
[66] Ferro G, Guarino F, Castiglione S, Rizzo L. Antibiotic resistance spread potential in urban wastewater effluents disinfected by UV/H_2O_2 process. Sci Total Environ 2016;560–561:29–35.
[67] Guo C, Wang K, Hou S, Wan L, Lv J, Zhang Y, et al. H_2O_2 and/or TiO_2 photocatalysis under UV irradiation for the removal of antibiotic resistant bacteria and their antibiotic resistance genes. J Hazard Mater 2017;323:710–8.
[68] Miranda AC, Lepretti M, Rizzo L, Caputo I, Vaiano V, Sacco O, et al. Surface water disinfection by chlorination and advanced oxidation processes: inactivation of an antibiotic resistant *E. coli* strain and cytotoxicity evaluation. Sci Total Environ 2016;554–555:1–6.
[69] Beretsou VG, Michael-Kordatou I, Michael C, Santoro D, El-Halwagy M, Jäger T, et al. A chemical, microbiological and (eco)toxicological scheme to understand the efficiency of UV-C/H_2O_2 oxidation on antibiotic-related microcontaminants in treated urban wastewater. Sci Total Environ 2020;744:140835.
[70] Gao R, Yu M, Xie J, Sui M. Inactivation of vancomycin-resistant *Enterococcus faecalis* and degradation of intracellular *vanB* gene under exposure to UV and UV/H_2O_2. J Water Process Eng 2022;49:103004.
[71] Michael-Kordatou I, Iacovou M, Frontistis Z, Hapeshi E, Dionysiou DD, Fatta-Kassinos D. Erythromycin oxidation and ERY-resistant *Escherichia coli* inactivation in urban wastewater by sulfate radical-based oxidation process under UV-C irradiation. Water Res 2015;85:346–58.
[72] Yao S, Hu Y, Ye J, Xie J, Zhao X, Liu L, et al. Disinfection and mechanism of super-resistant *Acinetobacter* sp. and the plasmid-encoded antibiotic resistance gene bla_{NDM-1} by UV/peroxymonosulfate. Chem Eng J 2022;433:133565.
[73] Berruti I, Nahim-Granados S, Abeledo-Lameiro MJ, Oller I, Polo-López MI. UV-C peroxymonosulfate activation for wastewater regeneration: simultaneous inactivation of pathogens and degradation of contaminants of emerging concern. Molecules 2021;26(16):4890.
[74] Zhang T, Lv K, Lu Q, Wang L, Liu X. Removal of antibiotic-resistant genes during drinking water treatment: a review. J Environ Sci 2021;104:415–29.
[75] Chen J, Loeb S, Kim JH. LED revolution: fundamentals and prospects for UV disinfection applications. Environ Sci Water Res Technol 2017;3(2):188–202.
[76] Li Y, Yang M, Zhang X, Jiang J, Liu J, Yau CF, et al. Two-step chlorination: a new approach to disinfection of a primary sewage effluent. Water Res 2017;108:339–47.
[77] Zhang Y, Chu W, Xu T, Yin D, Xu B, Li P, et al. Impact of pre-oxidation using H_2O_2 and ultraviolet/H_2O_2 on disinfection byproducts generated from chlor(am)ination of chloramphenicol. Chem Eng J 2017;317:112–8.
[78] Ferreira LC, Castro-Alférez M, Nahim-Granados S, Polo-López MI, Lucas MS, Li Puma G, et al. Inactivation of water pathogens with solar photo-activated persulfate oxidation. Chem Eng J 2020;381:122275.
[79] Wang D, Junker AL, Sillanpää M, Jiang Y, Wei Z. Photo-based advanced oxidation processes for zero pollution: where are we now? Engineering 2023;23:19–23.
[80] Li GQ, Huo ZY, Wu QY, Lu Y, Hu HY. Synergistic effect of combined UV-LED and chlorine treatment on *Bacillus subtilis* spore inactivation. Sci Total Environ 2018;639:1233–40.
[81] Chen L, Gao S, Lou L, Zhou Z. Removal of intracellular and extracellular antibiotic resistance genes from swine wastewater by sequential electrocoagulation and electro-Fenton processes. Environ Eng Sci 2021;38(2):74–80.
[82] Wang L, Ye C, Guo L, Chen C, Kong X, Chen Y, et al. Assessment of the UV/chlorine process in the disinfection of *Pseudomonas aeruginosa*: efficiency and mechanism. Environ Sci Technol 2021;55(13):9221–30.
[83] Liu Y, He X, Fu Y, Dionysiou DD. Degradation kinetics and mechanism of oxytetracycline by hydroxyl radical-based advanced oxidation processes. Chem Eng J 2016;284:1317–27.
[84] Xiao R, Liu K, Bai L, Minakata D, Seo Y, Kaya Göktaş R, et al. Inactivation of pathogenic microorganisms by sulfate radical: present and future. Chem Eng J 2019;371:222–32.
[85] Lu X, Shao Y, Gao N, Chen J, Zhang Y, Xiang H, et al. Degradation of diclofenac by UV-activated persulfate process: kinetic studies, degradation pathways and toxicity assessments. Ecotoxicol Environ Saf 2017;141:139–47.
[86] Khan S, He X, Khan JA, Khan HM, Boccelli DL, Dionysiou DD. Kinetics and mechanism of sulfate radical- and hydroxyl radical-induced degradation of

highly chlorinated pesticide lindane in UV/peroxymonosulfate system. Chem Eng J 2017;318(13):135–42.
[87] He X, de la Cruz AA, O'Shea KE, Dionysiou DD. Kinetics and mechanisms of cylindrospermopsin destruction by sulfate radical-based advanced oxidation processes. Water Res 2014;63:168–78.
[88] Duan X, Niu X, Gao J, Wacławek S, Tang L, Dionysiou DD. Comparison of sulfate radical with other reactive species. Curr Opin Chem Eng 2022;38:100867.
[89] Zhang Y, Zhao YG, Yang D, Zhao Y. Insight into the removal of tetracycline-resistant bacteria and resistance genes from mariculture wastewater by ultraviolet/persulfate advanced oxidation process. J Hazard Mater Adv 2022;7:100129.
[90] More TT, Yadav JSS, Yan S, Tyagi RD, Surampalli RY. Extracellular polymeric substances of bacteria and their potential environmental applications. J Environ Manage 2014;144:1–25.
[91] Fish K, Osborn AM, Boxall JB. Biofilm structures (EPS and bacterial communities) in drinking water distribution systems are conditioned by hydraulics and influence discolouration. Sci Total Environ 2017;593–594:571–80.
[92] Jia S, Shi P, Hu Q, Li B, Zhang T, Zhang XX. Bacterial community shift drives antibiotic resistance promotion during drinking water chlorination. Environ Sci Technol 2015;49(20):12271–9.
[93] Zhang Z, Li B, Li N, Sardar MF, Song T, Zhu C, et al. Effects of UV disinfection on phenotypes and genotypes of antibiotic-resistant bacteria in secondary effluent from a municipal wastewater treatment plant. Water Res 2019;157:546–54.
[94] McKinney CW, Pruden A. Ultraviolet disinfection of antibiotic resistant bacteria and their antibiotic resistance genes in water and wastewater. Environ Sci Technol 2012;46(24):13393–400.
[95] Nihemaiti M, Yoon Y, He H, Dodd MC, Croué JP, Lee Y. Degradation and deactivation of a plasmid-encoded extracellular antibiotic resistance gene during separate and combined exposures to UV_{254} and radicals. Water Res 2020;182:115921.
[96] Kalisvaart BF. Re-use of wastewater: preventing the recovery of pathogens by using medium-pressure UV lamp technology. Water Sci Technol 2004;50(6):337–44.
[97] Rattanakul S, Oguma K. Inactivation kinetics and efficiencies of UV-LEDs against *Pseudomonas aeruginosa, Legionella pneumophila*, and surrogate microorganisms. Water Res 2018;130:31–7.
[98] Soro AB, Whyte P, Bolton DJ, Tiwari BK. Modelling the effect of UV light at different wavelengths and treatment combinations on the inactivation of *Campylobacter jejuni*. Innov Food Sci Emerg Technol 2021;69:102626.
[99] Jing Z, Lu Z, Santoro D, Zhao Z, Huang Y, Ke Y, et al. Which UV wavelength is the most effective for chlorine-resistant bacteria in terms of the impact of activity, cell membrane and DNA? Chem Eng J 2022;447:137584.
[100] Pirnie JP, Linden M, Malley KG. Ultraviolet disinfection guidance manual for the final long term 2 enhanced surface water treatment rule. EPA 815-R-06–007. Washington, DC: US Environmental Protection Agency; 2006.
[101] Ghosh S, Chen Y, Hu J. Application of UVC and UVC based advanced disinfection technologies for the inactivation of antibiotic resistance genes and elimination of horizontal gene transfer activities: opportunities and challenges. Chem Eng J 2022;450:138234.
[102] Clarke S, Bettin W. Ultraviolet light disinfection in the use of individual water purification devices. Harford: U.S. Army Center for Health Promotion and Preventive Medicine; 2006.
[103] Wu Z, Guo K, Fang J, Yang X, Xiao H, Hou S, et al. Factors affecting the roles of reactive species in the degradation of micropollutants by the UV/chlorine process. Water Res 2017;126:351–60.
[104] Yeom Y, Han J, Zhang X, Shang C, Zhang T, Li X, et al. A review on the degradation efficiency, DBP formation, and toxicity variation in the UV/chlorine treatment of micropollutants. Chem Eng J 2021;424:130053.
[105] Yao S, Ye J, Xia J, Hu Y, Zhao X, Xie J, et al. Inactivation and photoreactivation of bla_{NDM-1}-carrying super-resistant bacteria by UV, chlorination and UV/chlorination. J Hazard Mater 2022;439:129549.
[106] Xiao Y, Zhang L, Zhang W, Lim KY, Webster RD, Lim TT. Comparative evaluation of iodoacids removal by UV/persulfate and UV/H_2O_2 processes. Water Res 2016;102:629–39.
[107] Ghodbane H, Hamdaoui O. Decolorization of antraquinonic dye, C.I. Acid Blue 25, in aqueous solution by direct UV irradiation, UV/H_2O_2 and UV/Fe(II) processes. Chem Eng J 2010;160(1):226–31.
[108] Cui C, Jin L, Jiang L, Han Q, Lin K, Lu S, et al. Removal of trace level amounts of twelve sulfonamides from drinking water by UV-activated peroxymonosulfate. Sci Total Environ 2016;572:244–51.
[109] Rehman F, Sayed M, Khan JA, Shah NS, Khan HM, Dionysiou DD. Oxidative removal of brilliant green by UV/$S_2O_8^{2-}$, UV/HSO_5^- and UV/H_2O_2 processes in aqueous media: a comparative study. J Hazard Mater 2018;357:506–14.
[110] Gao JF, Duan WJ, Zhang WZ, Wu ZL. Effects of persulfate treatment on antibiotic resistance genes abundance and the bacterial community in secondary effluent. Chem Eng J 2020;382:121860.
[111] Yang Y, Xu C, Cao X, Lin H, Wang J. Antibiotic resistance genes in surface water of eutrophic urban lakes are related to heavy metals, antibiotics, lake morphology and anthropic impact. Ecotoxicology 2017;26(6):831–40.
[112] Zhang S, Wang Y, Song H, Lu J, Yuan Z, Guo J. Copper nanoparticles and copper ions promote horizontal transfer of plasmid-mediated multi-antibiotic resistance genes across bacterial genera. Environ Int 2019;129:478–87.
[113] Qiu Q, Li G, Dai Y, Xu Y, Bao P. Removal of antibiotic resistant microbes by Fe(II)-activated persulfate oxidation. J Hazard Mater 2020;396:122733.
[114] Delcomyn CA, Bushway KE, Henley MV. Inactivation of biological agents using neutral oxone–chloride solutions. Environ Sci Technol 2006;40(8):2759–64.
[115] Zhang Y, Gu AZ, Cen T, Li X, He M, Li D, et al. Sub-inhibitory concentrations of heavy metals facilitate the horizontal transfer of plasmid-mediated antibiotic resistance genes in water environment. Environ Pollut 2018;237:74–82.
[116] Lee MY, Wang WL, Du Y, Hu HY, Huang N, Xu Z, et al. Enhancement effect among a UV, persulfate, and copper (UV/PS/Cu^{2+}) system on the degradation of nonoxidizing biocide: the kinetics, radical species, and degradation pathway. Chem Eng J 2020;382:122312.
[117] Cai A, Deng J, Zhu T, Ye C, Li J, Zhou S, et al. Enhanced oxidation of carbamazepine by UV-LED/persulfate and UV-LED/H_2O_2 processes in the presence of trace copper ions. Chem Eng J 2021;404:127119.
[118] Sichel C, Garcia C, Andre K. Feasibility studies: UV/chlorine advanced oxidation treatment for the removal of emerging contaminants. Water Res 2011;45(19):6371–80.
[119] Guo K, Wu Z, Yan S, Yao B, Song W, Hua Z, et al. Comparison of the UV/chlorine and UV/H_2O_2 processes in the degradation of PPCPs in simulated drinking water and wastewater: kinetics, radical mechanism and energy requirements. Water Res 2018;147:184–94.
[120] Wan Q, Wen G, Cao R, Xu X, Zhao H, Li K, et al. Comparison of UV-LEDs and LPUV on inactivation and subsequent reactivation of waterborne fungal spores. Water Res 2020;173:115553.
[121] Hong Kong Electrics. Non-residential tariff [Internet]. Hong Kong: HK Electric Investments Limited; undated [cited 2023 Jan 9]. Available from: https://www.hkelectric.com/en/customer-services/billing-payment-electricity-tariffs/non-residential-tariff.
[122] Xiang Y, Fang J, Shang C. Kinetics and pathways of ibuprofen degradation by the UV/chlorine advanced oxidation process. Water Res 2016;90:301–8.
[123] Miklos DB, Wang WL, Linden KG, Drewes JE, Hübner U. Comparison of UV-AOPs (UV/H_2O_2, UV/PDS and UV/chlorine) for TOrC removal from municipal wastewater effluent and optical surrogate model evaluation. Chem Eng J 2019;362:537–47.
[124] Rodríguez-Chueca J, Varella della Giustina S, Rocha J, Fernandes T, Pablos C, Encinas Á, et al. Assessment of full-scale tertiary wastewater treatment by UV-C based-AOPs: removal or persistence of antibiotics and antibiotic resistance genes? Sci Total Environ 2019;652:1051–61.
[125] Tian FX, Ye WK, Xu B, Hu XJ, Ma SX, Lai F, et al. Comparison of UV-induced AOPs (UV/Cl_2, UV/NH_2Cl, UV/ClO_2 and UV/H_2O_2) in the degradation of iopamidol: kinetics, energy requirements and DBPs-related toxicity in sequential disinfection processes. Chem Eng J 2020;398:125570.
[126] Li D, Feng Z, Zhou B, Chen H, Yuan R. Impact of water matrices on oxidation effects and mechanisms of pharmaceuticals by ultraviolet-based advanced oxidation technologies: a review. Sci Total Environ 2022;844:157162.
[127] Zhao Q, Shang C, Zhang X, Ding G, Yang X. Formation of halogenated organic byproducts during medium-pressure UV and chlorine coexposure of model compounds, NOM and bromide. Water Res 2011;45(19):6545–54.
[128] Hua Z, Li D, Wu Z, Wang D, Cui Y, Huang X, et al. DBP formation and toxicity alteration during UV/chlorine treatment of wastewater and the effects of ammonia and bromide. Water Res 2021;188:116549.
[129] Wang C, Moore N, Bircher K, Andrews S, Hofmann R. Full-scale comparison of UV/H_2O_2 and UV/Cl_2 advanced oxidation: the degradation of micropollutant surrogates and the formation of disinfection byproducts. Water Res 2019;161:448–58.
[130] Yang M, Zhang X. Comparative developmental toxicity of new aromatic halogenated DBPs in a chlorinated saline sewage effluent to the marine polychaete *Platynereis dumerilii*. Environ Sci Technol 2013;47(19):10868–76.
[131] Wagner ED, Plewa MJ. CHO cell cytotoxicity and genotoxicity analyses of disinfection by-products: an updated review. J Environ Sci 2017;58:64–76.
[132] Mitch WA, Richardson SD, Zhang X, Gonsior M. High-molecular-weight by-products of chlorine disinfection. Nat Water 2023;1(4):336–47.
[133] Richardson SD, Plewa MJ, Wagner ED, Schoeny R, DeMarini DM. Occurrence, genotoxicity, and carcinogenicity of regulated and emerging disinfection by-products in drinking water: a review and roadmap for research. Mutat Res 2007;636(1–3):178–242.
[134] Han JR, Zhang XR, Jiang JY, Li WX. How much of the total organic halogen and developmental toxicity of chlorinated drinking water might be attributed to aromatic halogenated DBPs? Environ Sci Technol 2021;55(9):5906–16.
[135] Han JR, Zhang XR. Evaluating the comparative toxicity of DBP mixtures from different disinfection scenarios: a new approach by combining freeze-drying or rotoevaporation with a marine polychaete bioassay. Environ Sci Technol 2018;52(18):10552–61.
[136] Luo Y, Feng L, Liu Y, Zhang L. Disinfection by-products formation and acute toxicity variation of hospital wastewater under different disinfection processes. Separ Purif Tech 2020;238:116405.